Upconversion luminescence and Judd-Ofelt analysis of Nd^{3+} ions in $BaGd_2ZnO_5$ microcrystals

T. ZHU, C. NIU, Y. LV*
School of Instrument Science and Opto Electronics Engineering, Beijing Information & Technology University, Beijing 100192, China

$BaGd_2ZnO_5$ microcrystalline powders with different Nd^{3+} doping concentrations were prepared by high temperature solid phase method. All products were confirmed to be pure phase of $BaGd_2ZnO_5$ by X-ray diffraction pattern analysis. The diffuse reflection spectrum of the microcrystalline powder was measured by an integrating sphere and the absorption spectrum was calculated. According to Judd-Ofelt theory, the spectral intensity parameters were calculated to be Ω_2=$0.42 \times 10^{-20} cm^2$, Ω_4=$1.14 \times 10^{-20} cm^2$, and Ω_6=$4.32 \times 10^{-20} cm^2$, respectively. The theoretical oscillator strength and experimental oscillator strength of the sample were also calculated and their deviation is 7.53×10^{-7}. Then, the transition probability, transition branch ratio and energy level lifetime of Nd^{3+} are obtained. The upconversion emission spectra under 808 nm excitation were measured and several significant upconversion emission peaks at 328 nm, 385 nm, 420 nm, 477 nm, 528 nm, 564 nm and 595 nm, were observed. Fitting relationship curve of upconversion intensity to LD working current, indicates that luminescence at 385 nm, 420 nm and 477 nm belongs to two-photon process. Concentration quenching effect has also been observed. The calculation of the CIE color coordinates shows that all the coordinates of the six samples located at blue-green region.

(Received July 4, 2019; accepted August 18, 2020)

Keywords: $BaGd_2ZnO_5$, Nd^{3+}, Judd-Ofelt theory, CIE coordinates

1. Introduction

The luminescent material generally consists of matrix and activating ions. The matrix provides a suitable crystal field for the activated ions to produce suitable luminescence. As an activating ion for generating laser, the rare earth Nd^{3+} ion has an ideal four-level system [1, 2]. It has a wide absorption band in the visible and near-infrared bands [3] and suitable absorption cross sections and emission cross sections. Therefore, Nd^{3+} doped materials have been extensively studied and used in the fields of optical waveguide amplifiers, laser, up-conversion luminescence, and optical communication [4-7].

The Nd^{3+} doped matrix needs good chemical stability and low phonon energy [8-11]. Due to the tensile vibration of the host lattice, phonon energy of oxide matrix is relatively high, generally greater than 500 cm^{-1}. But as one of oxide matrices, $BaGd_2ZnO_5$ has a lower phonon energy (about 360 cm^{-1}) [12-15]. Therefore, it is valuable to absorption property and fluorescence performance of Nd^{3+} doped $BaGd_2ZnO_5$ matrix.

Judd-Ofelt (J-O) theory has been widely used to calculate the spectral intensity parameters of rare earth ions in glassy and crystalline bodies [16, 17]. And J-O theory provides the possibility to analyze the crystal structure within a certain precision [18-20]. The J-O intensity parameters Ω_t (t = 2, 4, 6) are critical for evaluating performance of laser medium and up-conversion prosphor. However, for many microcrystalline powder materials, it is difficult to obtain basic physical parameters such as refractive index, doping concentration and absorption rate, utilizing J-O theory to research optical performance is limited.

In this paper, to our knowledge, spectral characteristics of Nd^{3+} ions in $BaGd_2ZnO_5$ microcrystalline powders were studied for the first time using J-O theory. Firstly, six samples of $BaGd_2ZnO_5$ microcrystalline powders with different Nd^{3+} doping concentrations were prepared by high temperature solid phase method, and their phase compositions were analyzed by X-ray diffraction (XRD). Secondly, the absorption spectrum was calculated by measuring the diffuse reflection spectrum of the microcrystalline powder sample, and spectral characteristics were calculated by J-O theory. Thirdly, the emission spectrum of the prepared sample under 808 nm excitation was measured, and the relationship between the emission peak intensity and the Nd^{3+} ion doping concentration was obtained. Then, by fitting up-conversion intensities curve to the pumping Laser Diode (LD) working current, it is found that the luminescence at 385 nm, 420 nm and 477 nm belong to two-photon processes. Finally, the CIE color coordinates of the six samples are calculated and discussed.

2. Judd-Ofelt theory

Judd [16] and Ofelt [17] developed a qualitative calculation method for the transition strength of rare earth ions independently, called Judd-Ofelt (J-O) theory.

In J-O theory, the strength of the electric dipole transition can be expressed as:

$$S_{ed} = \sum \Omega_t \left|\langle 4f^N \psi J \left\| U^{(t)} \right\| 4f^N \psi' J' \rangle\right|^2 (t = 2,4,6), \quad (1)$$

Here, $\left\|U^{(t)}\right\|$ is a unit tensor operator, $\left|\langle 4f^N \psi J \left\| U^{(t)} \right\| 4f^N \psi' J' \rangle\right|^2$ is reduced matrix element, which is related to the type and transition energy level of the rare earth ions but is independent of the host medium, and Ω_t is a spectral line intensity parameter, which is related to the lattice position of the rare earths ions in the host medium.

The experimental oscillator strength of the electric dipole transition can be expressed as:

$$f_{exp} = \frac{8\pi^2 mc}{3h(2J+1)\bar{\lambda}} \frac{(n^2+2)^2}{9n} S_{ed}, \quad (2)$$

Among them, m is the electron mass, h and c are the constant and the speed of light, J is the total angular quantum numbers of the initial transition energy level, $\bar{\lambda}$ is indicating the center wavelength of the absorption peak.

The spectral line strength of the magnetic dipole transition can be expressed as:

$$S_{md} = \frac{h^2}{16\pi^2 m^2 c^2} |< 4f^N \Psi J \| (\boldsymbol{L} + 2\boldsymbol{S}) \| \ 4f^N \Psi' J' >|^2, \quad (3)$$

Here, $|< 4f^N \Psi J \| (\boldsymbol{L} + 2\boldsymbol{S}) \| \ 4f^N \Psi' J' >|^2$ is the matrix element reduction of the magnetic dipole transition. The intensity of the line oscillator of the magnetic dipole transition can be expressed as:

$$f_{md} = \frac{hn}{6mc(2J+1)\bar{\lambda}} S_{md}. \quad (4)$$

For spectral transitions between two adjacent energy levels of rare earth ions, the experimental oscillator strength can be expressed as the sum of the electric dipole oscillator strength and the magnetic dipole oscillator strength, which is $f_{exp} = f_{ed} + f_{md}$. The magnetic dipole effect can be ignored compared to the electric dipole effect, $f_{exp} \approx f_{ed}$.

The experimental oscillator strength is related to the integral amount of each spectral absorption peak:

$$f_{exp} = \frac{mc^2}{\pi \bar{\lambda}^2 e^2 N} \int k(\lambda) d\lambda, \quad (5)$$

Here, e is the electric quantity of electrons. N is the dose concentration of rare earth ions (unit: cm^{-3}). $k(\lambda)$ is the optical density, which is related to the absorption coefficient $\alpha(\lambda)$:

$$k(\lambda) = \frac{\alpha(\lambda)}{0.43 \cdot l}, \quad (6)$$

Among them, l is the optical path length in the main medium.

According to equations (1), (2) and (5), the spectral intensity parameters, Ω_t, can be obtained by fitting the square of the absorption spectrum.

The theoretical oscillator strength can be expressed as:

$$f_{cal} = \frac{8\pi^2 mc}{3h(2J+1)\bar{\lambda}} \frac{(n^2+2)^2}{9n} S, \quad (7)$$

The transition ratio from the energy level Ψ_J to $\Psi'_{J'}$ is:

$$\beta[J, J'] = A_{JJ'} / [\sum_{J'} A_{JJ'}]. \quad (8)$$

The lifetime of an energy level Ψ_J is equal to the sum of spontaneous transitions from Ψ_J to all its lower levels, namely:

$$\tau = 1 / [\sum_{J'} A_{JJ'}]. \quad (9)$$

3. Experiment

3.1. Material preparation

Six pieces of 10g raw material, according to the molar ratio of $BaCO_3$: ZnO: Gd_2O_3: Nd_2O_3 = 100 : 105 : 100-x : x (x = 2, 4, 8, 16, 24, 32), were weighed. Among them, the excess 5% ZnO is to compensate for the loss of Zn^{2+} ions generated by pyrolysis of ZnO, Gd_2O_3 and Nd_2O_3 are spectrally pure reagents, and $BaCO_3$ and ZnO are analytically pure reagents.

Six pieces of raw materials are sequentially ground in an agate mortar to mix evenly, and then placed in six 15 ml small ceramic crucibles. Outside the six small ceramic crucibles, six large ceramic crucibles were covered for preventing volatilization of raw materials, then were placed in a muffle furnace, calcined at 1200 °C for 4 hours, then taken out and naturally cooled to room temperature. The cooled samples were again ground and packaged in six sample bags for the next measurement. The six

prepared samples were numbered as 1#(x = 2), 2#(x = 4), 3#(x = 8), 4#(x = 16), 5#(x = 24) and 6# (x = 32), respectively.

3.2. Measurement of material properties

Phase analysis was performed using a Hitachi DMAX-3A X-ray diffraction (XRD) with a scan range from 10° to 80°.

The excitation spectrum and the emission spectrum were measured using a Zolix Omi-λ150 monochromator, an Omi-λ300 monochromator and a PMTH-S1-CR131 photomultiplier, and an 808 nm LD laser.

The diffuse reflectance spectra were measured using an Avantes ASPHERES-50-LS-HAL-12V integrating sphere and an AvaSpec-2018 fiber spectrometer. According to the references [21], the absorption spectrum can be obtained from the diffuse reflection spectrum of Nd^{3+} ions in $BaGd_2ZnO_5$ microcrystalline powders.

4. Results and analysis

4.1. XRD analysis

The XRD pattern of 6# sample is shown in Fig. 1. It can be seen from Fig. 1 that the main XRD peak is consistent with the X-ray diffraction peak of the crystalline $BaGd_2ZnO_5$ in the 49-0518th PDF card, indicating that $BaCO_3$, ZnO and Gd_2O_3 react completely to form $BaGd_2ZnO_5$.

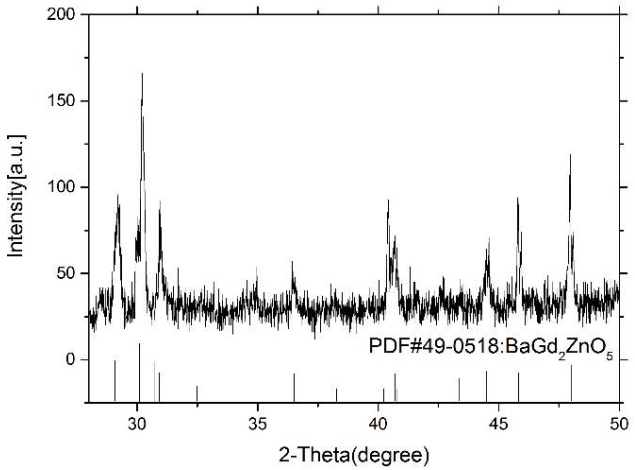

Fig. 1. XRD pattern of sample 6#

4.2. Absorption Spectrum and J-O Calculation

The absorption spectrum of the prepared sample 6# was measured by the measurement method described above, as shown in Fig. 2.

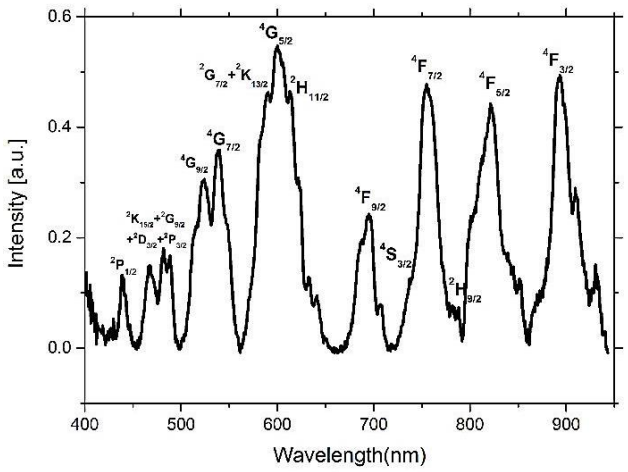

Fig. 2. Absorption spectrum of sample 6#

Fig. 2 shows that Nd^{3+} ions have many outstanding absorption peaks in the spectral range from 400 nm to 950 nm, which correspond to the transition of the $^4I_{9/2}$ state to the different excited states of the 4*f* shell electrons in Nd^{3+} ions. The energy levels of the excited states corresponding to the respective absorption bands are shown. It can also be seen from Fig. 2 that the absorption peak of the transition between $^4I_{9/2}\rightarrow{}^4I_{5/2}$ and $^4I_{9/2}\rightarrow{}^4H_{9/2}$ is around 808 nm, which is the output wavelength of commercialized LD.

For the powder sample, its refractive index n, ion doping concentration N and optical absorption length d are not directly available. According to reference [22], the refractive index n of the powder host material can be derived from the emission spectrum and the $^5D_0$ lifetime of the Eu^{3+} ions doped in the powder host material.

If the magnetic dipole transition probability of the $^5D_0\rightarrow{}^7F_1$ conversion is A_1, the other transitions ($^5D_0\rightarrow{}^7F_j$ (j = 0, 2, 3, 4, 5, 6) can be described as $A_j=a_jA_1$, here, $a_j = \frac{\int I_j(\nu)d\nu}{\int I_1(\nu)d\nu}\cdot\frac{\bar{\nu}_1}{\bar{\nu}_j}$, it is the ratio of the integrated peak intensity of the other transition to the integrated peak intensity of the transition of $^5D_0\rightarrow{}^7F_1$. The magnetic dipole transition probability A_1 can be calculated as $A_1 = \frac{1}{\tau_0\cdot\left(\sum_{j=0}^{6} a_j\right)}$, where τ_0 is the lifetime of the $^5D_0$ energy level of the Eu^{3+} ion [23].

If the refractive index n' and magnetic dipole transition probability A'_1 are known, the refractive index n of the powder host material can be expressed as $n = n'\cdot(A_1/A'_1)^{1/3}$。

The refractive index of $BaGd_2ZnO_5$ powder host material is derived as 2.31.

Furthermore, according to the reference [24], simulation results using multiple diffuse reflection methods show that the optical path in the powder material is proportional to the refractive index, and the optical path length increases by 15% in the refractive index range of 1.1 to 2.4. Because the measured absorption rate of 6# sample (n=2.31) is equal to absorption rate of borosilicate glass powder (n=1.7) with 0.94cm thickness, the actual optical path length of 6# sample is $d = 0.94cm \times (1 + 6.5\%) \cong 1.00cm$.

The ion doping concentration N is derived from the XRD data. The three parameters of the Nd^{3+} doped $BaGd_2ZnO_5$ microcrystalline powder sample are as follows, $n = 2.31, N = 3.04 \times 10^{20} cm^{-3}, d \approx 1.00cm$.

The absorption peak cross section area of the energy level transition is calculated by the absorption spectrum shown in Fig. 2.

According to equations (1), (2) and (5), the spectral intensity parameters, Ω_t, can be obtained by fitting the square of the absorption spectrum. The spectral intensity parameters of Nd^{3+} in $BaGd_2ZnO_5$ crystallites were calculated as, $\Omega_2 = 0.42 \times 10^{-20} cm^2$, $\Omega_4 = 1.14 \times 10^{-20} cm^2$ and $\Omega_6 = 4.32 \times 10^{-20} cm^2$.

Experimental oscillator strength and theoretical oscillator strength of Nd^{3+} ions transitions of for $^4I_{9/2} \rightarrow {}^2P_{1/2}$; $^4I_{9/2} \rightarrow {}^2K_{15/2}({}^2G_{9/2}, {}^2D_{3/2}, {}^2P_{3/2})$; $^4I_{9/2} \rightarrow {}^4G_{9/2}({}^4G_{7/2})$; $^4I_{9/2} \rightarrow {}^2G_{7/2}({}^2K_{13/2}, {}^4G_{5/2}, {}^2H_{11/2})$; $^4I_{9/2} \rightarrow {}^4F_{9/2}$; $^4I_{9/2} \rightarrow {}^4S_{3/2}$ $({}^4F_{7/2})$; $^4I_{9/2} \rightarrow {}^4F_{5/2}$; $^4I_{9/2} \rightarrow {}^4F_{3/2}$ are calculated and shown in Table 1.

The difference between the experimental oscillator strength and the theoretical oscillator strength can be expressed as:

$$\delta_{rms} = \left[\sum (\Delta f)^2 / \left(N_{tran} - N_{para}\right)\right]^{1/2} \qquad (10)$$

Here, $\sum(\Delta f)^2$ is the sum of the squares of the deviations between the experimental and theoretical oscillator strengths, N_{tran} is the number of observed energy level transitions caused by absorption, and N_{para} is the number of calculated parameters.

Table 1. Experimental and theoretical oscillator strength

Excited Energy Level	Center Wavelength (nm)	Experimental Oscillator strength $f_{ex}(\times 10^{-6})$	Theory Oscillator strength $f_{theo}(\times 10^{-6})$
$^2P_{1/2}$	440	0.52	0.27
$^2K_{15/2}$,$^2G_{9/2}$, $^2D_{3/2}$,$^2P_{3/2}$	475	1.75	0.99
$^4G_{9/2}$, $^4G_{7/2}$	530	4.21	3.64
$^2G_{7/2}$,$^2K_{13/2}$, $^4G_{5/2}$, $^2H_{11/2}$	607	7.19	7.21
$^4F_{9/2}$	684	1.02	0.78
$^4S_{3/2}$,$^4F_{7/2}$	752	11.56	10.84
$^4F_{5/2}$	808	7.65	8.68
$^4F_{3/2}$	899	2.05	1.56
$\boldsymbol{\delta}$		7.53×10^{-7}	

It can be seen from Table 1 that difference between the experimental oscillator strength and theoretical oscillator strength calculated by J-O theory is small, and root mean square deviation is $\delta_{rms} = 7.53 \times 10^{-7}$.

In the Nd^{3+}-doped laser matrix, outputting 1064 nm laser intensity is related to the radiative lifetime of the metastable $^4F_{3/2}$ energy level, and longer lifetime of $^4F_{3/2}$ can achieve higher inverted population. The transition probability, transition branch ratio and energy level lifetime of Nd^{3+} in the electric dipole approximation mode from the upper level $^4F_{3/2}$ to the lower level $^4I_{9/2}$,$^4I_{11/2}$,$^4I_{13/2}$,$^4I_{15/2}$ are calculated by equations (7) - (9), as shown in Table 2.

Table 2. Nd^{3+} transition probability, transition branch ratio and energy level lifetime

Energy level transition	Center wavelength (nm)	Transition probability $A_{JJ'}(s^{-1})$	Transition branch ratio $\boldsymbol{\beta}$ (%)	Energy level life τ_{rad}/ms
$^4F_{3/2}\rightarrow{}^4I_{9/2}$	870	1910.51	27.82	0.14
$^4I_{11/2}$	1065	3967.17	57.77	
$^4I_{13/2}$	1343	943.62	13.74	
$^4I_{15/2}$	1880	45.43	0.66	

In laser design, transition branch ratio is an important parameter, which characterizes probability of acquiring the stimulated emission of a certain energy level transition. It can be seen from Table 2 that branch ratio of transition $^4F_{3/2}\rightarrow{}^4I_{11/2}$ is the highest, 57.77%, and the corresponding wavelength is 1065 nm. Moreover, $^4F_{3/2}$ energy level has a long lifetime of 0.14 *ms*, and is suitable as an intermediate energy level for up-conversion luminescence.

4.3. Up-conversion Luminescence

In up-conversion luminescence experiment, an 808 nm LD with threshold current $i_0 = 0.42A$ is used as exciting light source.

The emission spectrum of six samples with different Nd^{3+} doping concentrations were collected under 808nm excitation, as shown in Fig. 3.

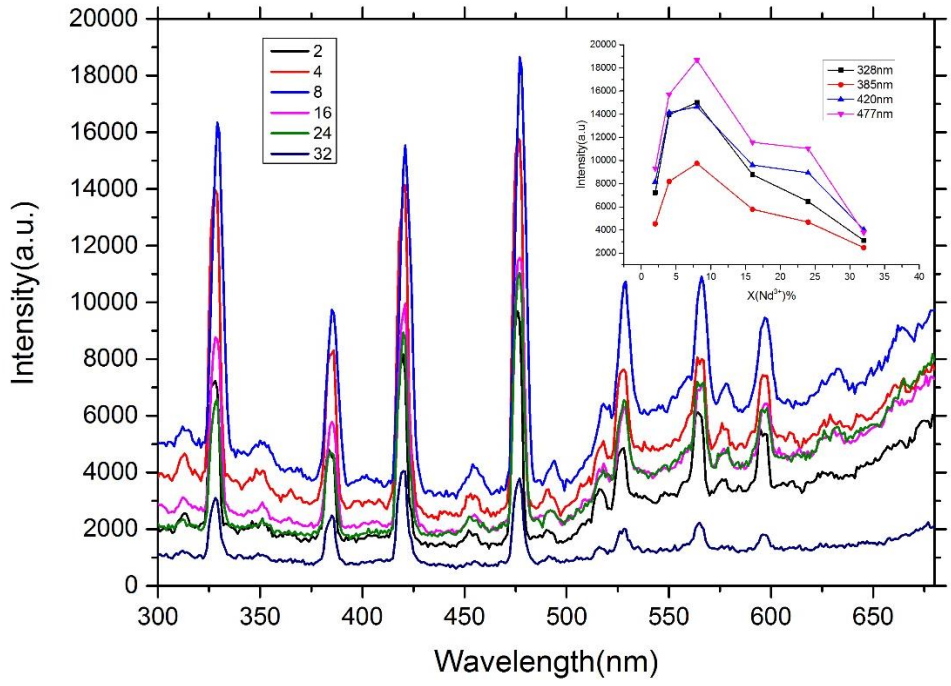

Fig. 3. Up-conversion emission spectra of different Nd^{3+} doping concentrations (color online)

(Inlet: luminescence vs doping concentration of Nd^{3+} ions)

It is apparent that six samples have similar up-conversion emission peaks, located at 328 nm, 385 nm, 420 nm, 477 nm, 528 nm, and 564 nm, respectively. The seven up-conversion luminescence correspond to $^2D_{5/2}\rightarrow{}^4I_{9/2}$, $^2P_{1/2}\rightarrow{}^4I_{9/2}$, $^2D_{3/2}\rightarrow{}^4I_{9/2}$, $^4G_{9/2}\rightarrow{}^4I_{9/2}$, $^2G_{7/2}\rightarrow{}^4I_{9/2}$, $^4G_{5/2}\rightarrow{}^4I_{9/2}$ of Nd^{3+} ions, respectively.

Furthermore, the relationship curves between luminescence intensity at emission peaks of 328 nm, 385 nm, 420 nm and 477 nm and the doping concentration of Nd^{3+} ions were plotted in the inset of Fig. 3. It is obvious that at the beginning, up-conversion emission intensities

increase with Nd^{3+} ions doping concentration increasing, and then up-conversion intensities decrease after doping concentration larger than 8%. In other words, a concentration quenching effect happens and 8% is the best doping concentration of Nd^{3+} ions in $BaGd_2ZnO_5$ microcrystalline.

According to the Dexter theory [25], in non-conductive inorganic materials, the concentration quenching mechanism of activator ions belongs to electrical multipole interactions. When doping concentration of activator ions in the phosphor is sufficiently large, the intensity of the luminescence is related to the mole fraction of the activator ions,

$$lg(I/x) = c - k \cdot lg(x), \tag{11}$$

here, I is the luminous intensity, x indicates the mole fraction of activator ions, k is a proportional coefficient, and c is a constant.

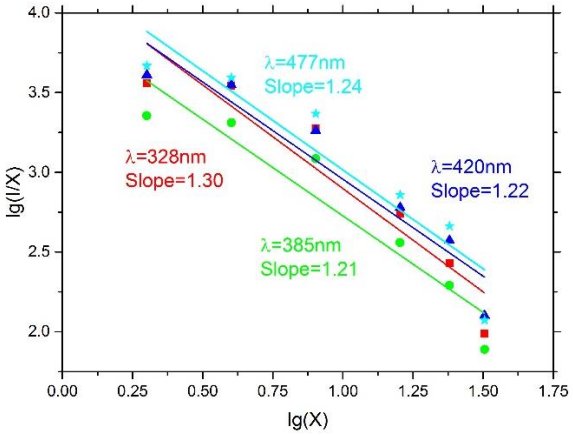

Fig. 4. $lg(I/x)$ and $lg(x)$ curve (color online)

The relationship curve between $lg(I/x)$ and $lg(x)$ is shown in Fig. 4. The dotted line indicates the fitted curve, and it is apparent that the slopes of the three fitting curves are 1.30 (328 nm), 1.21 (385 nm), 1.22 (420 nm), and 1.24 (477 nm), respectively. This means that concentration quenching mechanism of all the transitions of Nd^{3+} ion belong to dipole-dipole interaction.

Generally, up-conversion luminescence intensity has the following relationship with the laser light intensity [26]:

$$I_{lumin} = C \cdot I_{exit}^{n}, \tag{12}$$

where C is a constant and n is number of absorbed photons, for example, $n = 2$ means two-photon absorption, and $n = 3$ means three-photon absorption.

Usually, output power of a laser diode (LD) is proportional to the operating current within normal operating range,

$$I_{exit} = k \times (i - i_0) \tag{13}$$

here, k is the proportional coefficient related to performance of the laser diode, and i_0 indicates threshold current of LD, i is working current of the LD.

Substituting Equation (13) into equation (12), relation-ship between up-conversion luminescence intensity and LD operating current can be expressed as

$$I_{lumin} = C \cdot k^n \cdot (i - i_0)^n, \tag{14}$$

Taking logarithm of two sides of Eq. (14), there exist

$$ln(I_{lumin}) = lnC + ln(k^n) + ln(i - i_0)^n \tag{15}$$

The formula is a straight line equation, and the slope of straight line is the number of absorbed photon n.

In Fig. 5, experimental data of three up-conversion peaks at 385 nm, 420 nm, and 477 nm were fitted. The dots represent experimental data and the solid lines depict fitting results.

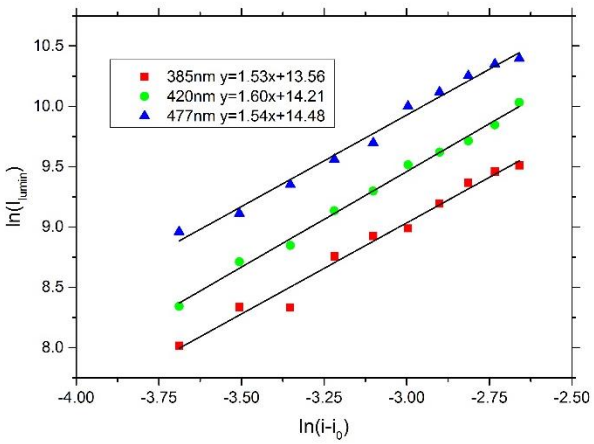

Fig. 5. 808 nm LD pump current VS. up conversion luminescence intensity (color online)

From the fitting results in Fig. 5, it can be seen that the slopes of three up-conversion transition peaks located at 385 nm, 420 nm and 477 nm are 1.53, 1.60 and 1.54, respectively, which means that the three up-conversion luminescence are two-photon processes.

4.4. CIE color coordinate

To investigate luminescence properties of the prepared samples, CIE coordinates of six prepared samples excited at 808 nm were calculated as shown in Table 3.

Table 3. CIE color coordinates of BaGd2ZnO5: Nd^{3+} phosphor under 808 nm excitation

Number	*X*	*Y*
1	0.3234	0.3279
2	0.3209	0.3254
3	0.3181	0.3217
4	0.3130	0.3151
5	0.3123	0.3141
6	0.3108	0.3118

It can be seen that CIE coordinates vary with doping concentration of Nd^{3+} ions, and all the CIE coordinate locate near (0.31, 0.31).

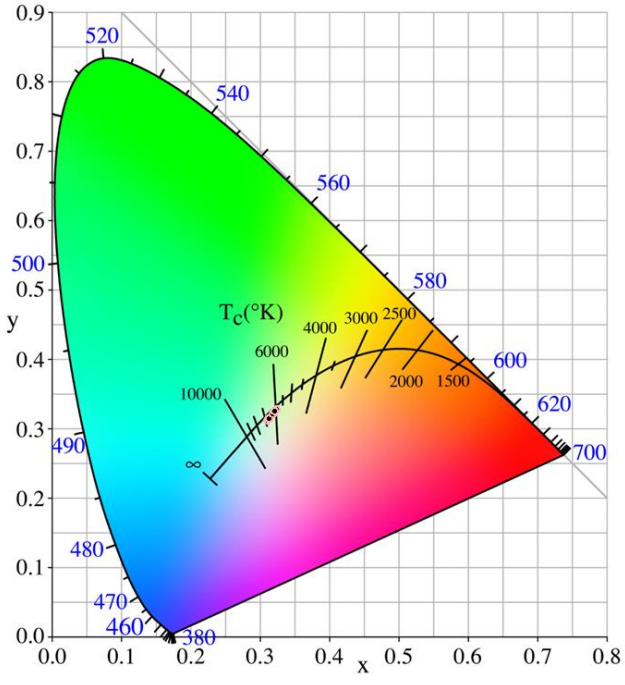

Fig. 6. CIE plot of samples with different Nd^{3+} doping concentrations (color online)

Fig. 6 is CIE plot of six prepared samples with different Nd^{3+} doping concentrations. It can be seen from Fig. 6 that luminescence of six samples are in the blue-green region. By calculation, CIE coordinate of sample #1 (Nd^{3+} doping concentration is 2%) is closest to white light region.

5. Conclusion

In conclusion, Nd^{3+} doped $BaGd_2ZnO_5$ microcrystalline powder are prepared through high-temperature solid phase method. XRD analysis indicates that the prepared compounds are well crystallized. Absorption spectrum are obtained and spectral characteristic are analyzed through Judd-Ofelt theory. The calculated spectrum intensity para-meters of the prepared sample are, $\Omega_2 = 0.42 \times 10^{-20} cm^2$, $\Omega_4 = 1.14 \times 10^{-20} cm^2$ and $\Omega_6 = 4.32 \times 10^{-20} cm^2$, respectively. The transition probability, branching ratio and energy level lifetime of Nd^{3+} ion in $BaGd_2ZnO_5$ micro-crystalline powder sample are computed and the results discover that $BaGd_2ZnO_5$ is a good up-conversion luminescence host material. Moreover, up-conversion spectrum under 808nm excitation are measured, emission peaks of purple light near 385 nm and blue light near 420 nm and 477 nm are observed, both of up-conversion luminescence belong to two photon absorbing process. Finally, the calculation of the CIE color coordinates shows that all the coordinates of the six samples located at blue-green region.

References

[1] G. Tang, Z. H. Xiao, C. G. Zuo, L. G. Han. Mater. Rev. **23**(6), 40 (2009) (in Chinese).
[2] S. Y. Zhang, Spectroscopy of Rare Earth Ions. Beijing: Science Publisher (2008) (in Chinese).
[3] Q. Shi, H. Cheng, J. W. Lv, Y. Sun, Chin. J. Lumin. **26**(3), 359 (2005) (in Chinese).
[4] Z. H. Jiang, Chin. J. Lasers **33**(9), 1265 (2006) (in Chinese).
[5] S. G. Xiao, Z. W. Liu, Spectrosc. Spect. Anal. **20**(4), 465 (2000) (in Chinese).
[6] Y. Huang, W. T. Li, L Zhang, D. P. Chen, W. Chen, L. L. Hu, Acta Opt. Sinica. **43**(10), 1006001-1-5 (2014) (in Chinese).
[7] J. T. Hua, B. J. Chen, J. S. H. Sun, L. H. Cheng, H. Y. Zhong, Chinese Optics. **03**(4), 301 (2010) (in Chinese).
[8] P. A. Loiko, O. S. Dymshits, I. P. Alekseeva, A. A. Zhilin, M. Y. Tsenter, E. V. Vilejshikova, K. V. Bogdanov, X. Mateos, K. V. Yumashev, Journal of Luminescence **179**, 64 (2016).
[9] S. Singh, S. P. Khatkar, R. Arora, D. Sangwan, A. Khatkar, V. B. Taxak, Journal of Electronic Materials **43**(4), 1175 (2014).
[10] Y. M. Yang, F. Y. Jiao, W. Zhang, J. P. Jiao, Z. Q. Li, X. Y. Su, N. Wen, Journal of Alloys and Compounds **567**, 107 (2013).
[11] Y. M. Yang, C. H. Mi, X. Y. Su, F. Y. Jiao, L. L. Liu, J. Zhang, F. Yu, X. D. Li, Y. Z. H. Liu, Y. H. Mai, Optics Letters **39**(7), 2000 (2014).
[12] B. Tian, B. Chen, Y. Tian, J. S. Sun, X. P. Li, J. S. Zhang, H. Y. Zhong, L. H. Cheng, Z. H. L. Wu, R. N.

Hua, Ceramics International **38**(5), 3537 (2012).
[13] B. N. Tian, Dalian Maritime University (2013) (in Chinese).
[14] Y. M. Yang, L. L. Liu, S. H. ZH. Cai, F. Y. Jiao, C. H. Mi, X. Y. Su, J. Zhang, F. Yu, X. D. Li, Z. Q. Li, Journal of Luminescence **146**, 284 (2014).
[15] A. Birkel, A. A. Mikhailovsky, A. K. Cheetham, Chemical Physics Letters **477**(54), 325 (2009).
[16] B. R. Judd, Phys. Rev. **127**, 750 (1962).
[17] G. S. Ofelt, J. Chem. Phys. **37**, 511 (1962).
[18] Q. L. Zhang, W. He, D. L. Sun, A. H. Wang, ZH. T. Yin, Spectroscopy and Spectral Analysis **03**, 329 (2005) (in Chinese).
[19] C. Manjunath, M. S. Rudresha, B. M. Walsh, R. Hari Krishna, B. S. Panigrahi, B. M. Nagabhushana, Dyes and Pigments **148**, 118 (2018).
[20] F. Hu, X. R. Liu, R. R. Chen, Y. ZH. Liu, Y. H. Mai, M. Ramzi, Y. M. Yang, Journal of Rare Earths **35**(10), 964 (2017).
[21] C. H. Niu, Y. J. Deng, Journal of Luminescence **204**, 528 (2018).
[22] X. Y. Jiang, Z. L. Zhang, S. H. Xu, Chin. J. Lumin. **11**, 80 (1990) (in Chinese).
[23] C. H. Niu, T. Zhu, Opt. Mater. **88**, 570 (2019).
[24] Z. L. Zhang, X. Y. Jiang, S. H. Xu, Acta Optica Sin. **11**, 312 (1991).
[25] D. L. Dexter. J. Chem. Phys. **21**, 836 (1953).
[26] M. Pollnau, D. R. Gamelin, S. R. Luthi, H. U. Gudel, Phys. Rev. B **61**, 3337 (2000).

*Corresponding author: lvyong@bistu.edu.cn